

4. CONCLUSION

In this article, we have presented a novel optoelectronic system with image encoding technique for invariant color pattern recognition based on the nonzero order joint transform correlation. Compared to multi-channel JTC in the joint input plane, the proposed IEJTC is easier and the system is smaller since three color channels of input image can be reduced to a single channel. For real-time processing, the joint input plane is displayed on the LCSLMs. In the tests, the algorithm is robust to in-plane rotation and noisy target images. It is expected that the proposed method is promising in color image recognition. To sum up, the overall performance is good in our system.

ACKNOWLEDGMENT

This research is supported by a research grant from the National Science Council of Taiwan (ROC) under contract NSC 95-2221-E-155-081.

REFERENCES

1. A. Vanderlugt, Signal detection by complex spatial filtering, *IEEE Trans Inform Theory* IT-10 (1964), 139–146.
2. C.S. Weaver and J.W. Goodman, A technique for optically convolving two functions, *Appl Opt* 5 (1966), 1248–1249.
3. F.T.S. Yu, G. Lu, M. Lu, and D. Zhao, Application of position encoding to complex joint transform correlator, *Appl Opt* 34 (1995), 1386–1388.
4. B. Javidi and C.J. Kuo, Joint transform image correlation using a binary spatial light modulator at the Fourier plane, *Appl Opt* 27 (1988), 663–665.
5. C. Chen, C. Chen, C. Lee, and C. Chen, Constrained optimization on the nonzero-order joint transform correlator with the Mach-Zehnder configuration, *Opt Commun* 231 (2004), 165–173.
6. G. Lu, Z. Zhang, S. Wu, and F.T.S. Yu, Implementation of a nonzero order joint transform correlator by use of phase shifting techniques, *Appl Opt* 36 (1997), 470–483.
7. C. Li, S. Yin, and F.T.S. Yu, Nonzero-order joint transform correlator, *Opt Eng* 37 (1998), 58–65.
8. C. Wu, C. Chen, and J. Fang, Constrained optimization for color pattern recognition with a nonzero order joint transform correlator, *Microwave Opt Technol Lett* 33 (2002), 385–388.
9. C. Chen and J. Fang, Chinese seal imprint recognition with joint transform correlators, *Opt Eng* 40 (2001), 2159–2164.
10. C. Lee and C. Chen, A Mach-Zehnder nonzero order joint transform correlator for aircraft pattern recognition, *Microwave Opt Technol Lett* 48 (2006), 1290–1293.
11. A. Mahalanobis, B.V.K.V. Kumar, and D. Casasent, Minimum average correlation energy filters, *App Opt* 26 (1987), 3633–3640.
12. M. Deutsch, J. Garcia, and D. Mendlovic, Multi-channel single-output color pattern recognition by use of a joint-transform correlator, *Appl Opt* 35 (1996), 6976–6982.
13. C. Wu and C. Chen, Performance comparison between multichannel polychromatic and conventional joint transform correlators, *Opt Eng* 42 (2003), 1758–1765.
14. C. Wu, C. Chen, and J. Fang, Linearly constraint color pattern recognition with a non-zero order joint transform correlator, *Opt Commun* 214 (2002), 65–75.
15. Y. Lin, C. Chen, and C. Lee, Mach-Zehnder joint transform correlator with multi-channel quantized reference functions for color pattern recognition, *Opt Commun* 266 (2006), 111–116.

© 2007 Wiley Periodicals, Inc.

TWO-DIMENSIONAL EFFICIENT METAMATERIAL-INSPIRED ELECTRICALLY-SMALL ANTENNA

Aycan Erentok and Richard W. Ziolkowski

Department of Electrical and Computer Engineering, The University of Arizona, 1230 E. Speedway Blvd., Tucson, AZ 85721-0104

Received 28 November 2006

ABSTRACT: *Inexpensive, efficient, and electrically-small antenna designs are presented, which are based on a two-dimensional (2D) metamaterial-inspired structure driven by an electrically-small rectangular semiloop antenna that is coaxially-fed through a finite PEC ground plane. Measured reflection coefficients showed a very good agreement with the simulated data, where the measured resonant frequency is only 0.5% different from the numerically predicted value. The proposed 2D antenna systems are linearly scalable with frequency, and predicted radiation characteristics of the antenna systems at 300, 430, and 1580 MHz are reported. © 2007 Wiley Periodicals, Inc. Microwave Opt Technol Lett 49: 1669–1673, 2007; Published online in Wiley InterScience (www.interscience.wiley.com). DOI 10.1002/mop.22542*

Key words: *metamaterials; electrically small antennas; loop antennas; antenna theory*

1. INTRODUCTION

An inexpensive, easy to build, efficient, and electrically-small antenna system that is naturally impedance matched to a source and is scalable to a wide range of frequencies without any compromise in its performance would be ideal for the new generation of wireless communications and sensor networks. The desired antenna performance requirements, however, are contradictory when standard electrically-small antenna designs are considered. In particular, electrically-small electric dipole or magnetic loop antennas are known to be inefficient radiators when they are fed by a 50 Ω source because they have a very small radiation resistance with large reactance differences from this source and, hence are very poorly matched to it.

Metamaterials (MTMs) are artificial materials that have engineered electromagnetic responses and that are not readily available in nature. Recent theoretical and experimental studies have shown that MTMs provide an alternate design methodology to improve the performance characteristics of several radiating and scattering systems [1]. These MTM-based antennas have been designed using spherical shells conceptualized with idealized MTMs [2]. For instance, electrically-small electric dipole and magnetic loop antennas radiating, respectively, in the presence of an electrically-small isotropic, homogenous, and dispersive (lossless and lossy) ϵ -negative (ENG) and a μ -negative (MNG) spherical shell(s) have been proposed. They have been shown both theoretically and numerically to produce efficient electrically-small antenna systems [2, 3].

This article reduces the earlier proposed three-dimensional EZ antenna system [4] to a planar antenna design by introducing an interdigitated capacitor. The 2D MTM-inspired element is designed to be resonantly driven by a rectangular semiloop antenna fed through a finite-sized ground plane with a 50 Ω coax feedline. It will be demonstrated that the resulting planar antenna system is naturally matched to the source and, hence, is an efficient radiator. It will also be shown that it acts as a resonant electrically-small magnetic dipole over a perfect electrically conducting (PEC) ground plane. The performance of the reported antenna system was simulated with Ansoft's High Frequency Structure Simulator

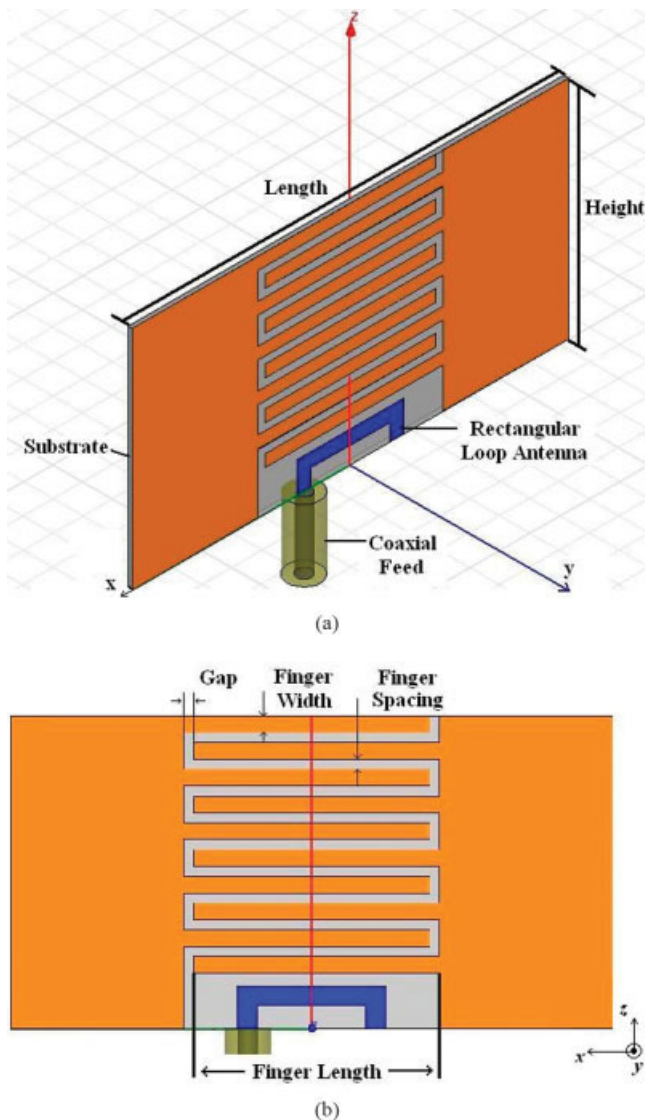


Figure 1 2D EZ antenna geometry and detailed specifications of each design variable for the 10-finger design. [Color figure can be viewed in the online issue, which is available at www.interscience.wiley.com]

(HFSS). Several of these 2D EZ antennas were fabricated, and the experimental results were compared to the simulations.

2. DESIGNS AND NUMERICAL RESULTS

A three-dimensional (3D) EZ antenna system was presented previously in Ref 4. An efficient, electrically-small antenna was methodology designed that utilized a capacitive structure that was

resonantly driven by an electrically-small semicircular loop antenna, the loop being coaxially-fed through a finite PEC ground plane. A capacitive element, which was a capacitively loaded loop (CLL) extruded along the direction orthogonal to the loop, provided the means to match the entire antenna system to the feedline and to tune its operating frequency.

The 2D planar version of the EZ antenna removes the third dimension of the original design, by using instead, a planar interdigitated capacitor for the CLL element. The design specifications of the proposed two-dimensional EZ antenna with its planar meta-material-inspired matching/radiating element are illustrated in Figure 1 and are summarized in Tables 1 and 2. The capacitor finger number, finger length, gap, and spacing between the fingers provide a tuning capability of the resonant frequency. The long and closely spaced capacitor fingers can be used to obtain lower resonant frequencies. The region between the bottom interdigitated capacitor finger and the ground plane captures the magnetic flux generated by the electrically-small semirectangular semiloop antenna that is driving it. The changes in time of this resonantly-large magnetic flux create induced currents on the CLL element, which produces a capacitance across the interdigitated finger spacings and gaps. The capacitance obtained from the induced currents is sufficiently large to match both the inductance due to the current path formed by the interdigitated CLL element and the copper ground plane, and the inductance of the electrically-small rectangular semiloop antenna. The planar interdigitated CLL element is a self-resonant reactive element that can be further matched to the reactance part of the electrically-small coax-fed rectangular semiloop antenna to create a resonant RLC tank circuit. The length, width, and height of the rectangular semiloop antenna also plays a major role in our ability to tailor the resistance and reactance of the radiating element to the 50 Ω coax feedline, thus achieving an efficient and electrically-small antenna system. In particular, a larger rectangular semiloop antenna enhances the resonant coupling of the driving antenna to the 2D interdigitated CLL element and thus, enhances the resulting radiation resistance and reactance of the system. The length and height (finger number, finger length, finger spacing, and finger gap) of the interdigitated CLL element provides the major inductance (capacitance) of this 2D antenna system. The width of the rectangular semiloop antenna contributes some to the inductance, but its overall effect to the tuning of the system is limited. The width of the rectangular semiloop, however, impacts the conductor losses in the antenna system.

We elected to design the planar antenna on a dielectric substrate only for fabrication purposes. In fact, using a dielectric substrate further introduces dielectric losses, which further decrease the overall efficiency of the antenna system. Moreover, low-loss dielectric substrates would increase the cost of the design. A planar EZ antenna based on a metal-only structure would produce the optimum 2D design. The 2D EZ antennas designed

TABLE 1 2D EZ Antenna Resonant Frequency Specifications, Rectangular Loop Antenna Details, Number of Interdigitated Capacitor Fingers, and Ground Plane Dimensions

Design	Antenna Length	Antenna	Antenna	Number of	Ground Plane
Frequency	Along x -Axis	Height Along	Width	Interdigitated	($x \times y$)
(MHz)	(mm)	z -Axis (mm)	(mm)	Capacitor Fingers	(mm ²)
Design 1 ^a	300	2	1.4	10	536 \times 536
Design 2	430	18	5.2	10	521 \times 521
Design 3	430	25	12	3	510 \times 510
Design 4	1580	5	3	3	137 \times 137

^a The copper conductivity value for this design was assumed to be 5.8E17 Simens/m.

TABLE 2 2D EZ Antenna Dimensions at 300, 430, and 1580 MHz

	Height Along z-Axis (mm)	Length along y-Axis (mm)	Finger Length Along x-Axis (mm)	Finger Width Along z-Axis (mm)	Finger Gap Along z-Axis (mm)	Finger Spacing Along z-Axis (mm)
Design 1 ^a	9.6	18	10.1	0.254	0.02	0.02
Design 2	38	73	29.8	2.032	1.2192	1.2192
Design 3	38	80	59.7	1.9	2.7	2.7
Design 4	10	22	10.5	0.7	0.15	0.15

^a The copper conductivity value for this design was assumed to be 5.8E17 Simens/m.

here used Rogers 5880 DuroidTM with a 31 mil (0.787 mm) thick substrate and a 0.5 oz. electrodeposited copper.

The HFSS model of the 2D EZ antenna consists of three components: (a) a rectangular semiloop copper antenna connected to a finite PEC ground plane and fed by a 50Ω coaxial-cable, (b) a predetermined number of interdigitated capacitor fingers that are uniformly positioned with the same gap and spacing across each element and with its two main “arms” being connected to the finite PEC ground plane, and (c) a vacuum radiation box that surrounds the antenna system. The default HFSS electrical properties were assigned for the copper, i.e., $\epsilon = \epsilon_0$, $\mu = \mu_0$, and $\sigma = 5.8 \times 10^{-8}$ S/m. The radiation box for each design was created using a half-cube that is at least a $\lambda/4$ distance away from the capacitive element per ANSOFT instructions, with the bottom face of the cube being assigned as the finite PEC ground plane. This requirement also fixes the size of the ground plane. Initial meshing was applied on the rectangular semiloop and on the interdigitated CLL element faces to improve the convergence of each simulation.

Tables 1 and 2 give the variable specifications of four different planar EZ antenna designs at three different frequencies: 300, 430, and 1580 MHz. Table 3 summarizes the HFSS predicted radiation characteristics of these 2D antenna systems. The calculation details of the computed radiated parameters were given in [4]. Design 1 was simulated using an extremely high conductivity metal and a lossless dielectric substrate to mimic an ideal lossless structure, and at 300 MHz it produced an overall efficiency of 99.7% with $ka = 0.085$, agreeing with the theoretical 3D EZ antenna radiation predictions [4]. The overall radiation efficiencies of the other 2D antenna systems with realistic copper and dielectric parameters depend on the electrical size of the antenna system. It decreases from nearly 90% at the electrically-small antenna limit $ka = 0.5$ to zero as the electrical size of the antenna system decreases. Design 2 was fabricated using a photolithography technique and was mounted on a 0.8 mm thick copper ground plane as shown in Figure 2(a). The simulated and measured S_{11} values of the fabricated Design 2 antenna system are given in Figure 2(b). The HFSS simulation 2 results given in Figure 2(b) are the predicted S_{11} values using exactly the same design parameters and dimensions, but with different convergence values from the HFSS simulation 1 results. The predicted resonance frequency of the antenna system with the more converged HFSS simulations, 435.89 MHz, was slightly above the original 430 MHz design value. The HFSS

simulation 2 data were obtained after we measured the fabricated structure and observed that the measured S_{11} values were somewhat different from the HFSS simulation 1 results. To explain the possible differences between the simulated and measured results, the HFSS simulations were rerun using more initial meshing on the design to obtain a maximum ΔS convergent value of 0.0005. The ΔS convergent value was 0.003 for the HFSS simulation 1 results. The measured S_{11} values showed a very good agreement with HFSS simulation 2 data, where the resonant frequency is only 0.5% different from the measured value of 438.1 MHz.

The planar EZ antenna dimensions are linearly scalable to any desired frequency, and this unique property can be seen from the frequency and component dimension ratios of Designs 3 and 4. The radiation efficiency comparisons of Designs 2 and 3 also show that the copper losses significantly impact the overall efficiency of the 2D EZ antenna system. This occurs because the system is highly resonant. Consequently, it is observed that an important practical criterion is to design the antenna system using a minimum number of interdigitated capacitor fingers to reduce the copper losses and, thus, to enhance the overall efficiency. The overall efficiencies of these electrically-small-limit systems are high and slightly less than the 3D EZ antenna predictions in Ref 4.

Figure 3(a) shows the far-field E- and H-field patterns obtained from Design 3 at 430.42 MHz. As these simulation results demonstrate, the 2D EZ antenna is acting like a magnetic dipole over a PEC ground plane. Figure 3(b) shows the current vector plots induced by the resonantly-large magnetic flux on the 2D interdigitated CLL element of Design 3 at the resonant frequency. A circulating current flow on the 2D interdigitated CLL element is clearly exhibited; this result supports the magnetic dipole over a PEC ground plane characteristics exhibited by the patterns in Figure 3(a).

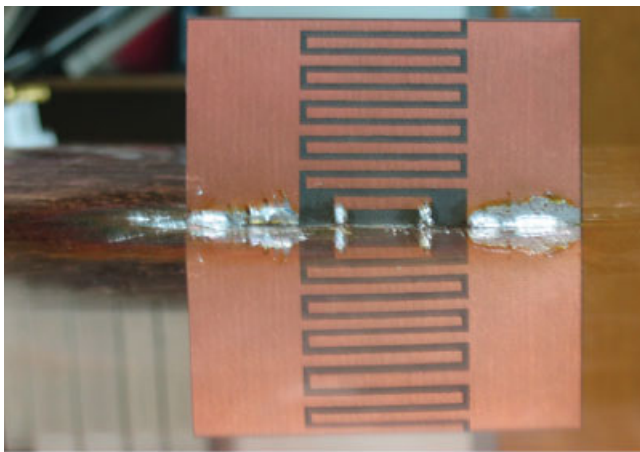
Comparisons of the 2D and 3D EZ antenna systems reveal that for the same design frequency, the 3D EZ antenna design is the more efficient choice between these two designs. The reduction of the extruded CLL element in the 3D EZ antenna design to the planar interdigitated CLL element in the 2D EZ antenna design reduces the amount and magnitude of the current flow on the CLL element and, consequently, reduces the radiation efficiency. The dielectric loss also contributes an increase of between 2% and 3% to the total loss of the 2D EZ overall efficiency depending on the frequency of operation.

TABLE 3 Summary of the 2D EZ Antenna Radiation Characteristics at 300, 430, and 1580 MHz

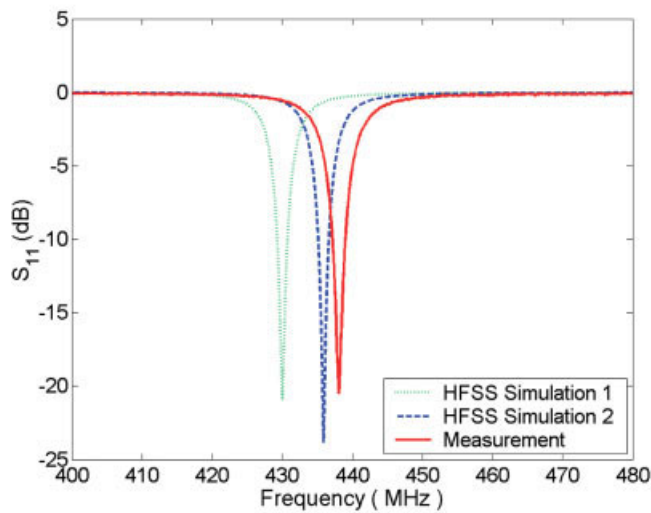
	F_{resonant} (MHz)	ka	FBW _{VSWR} (%)	Q/Q_{Chu}	AP (W)	RE (%)	OE (%)	D
Design 1 ^a	309.557	0.085	0.002	52.2	0.997	100	99.70	2.91
Design 2	430.02	0.475	0.347	63.2	0.992	80.14	79.50	3.78
Design 3	430.42	0.497	0.423	53.3	0.995	87.83	87.40	3.64
Design 4	1577.8	0.492	0.41	60.9	0.997	76.93	76.76	3.66

^a The copper conductivity value for this design was assumed to be 5.8E17 Simens/m.

ka , maximum electrical size of the antenna system; AP, accepted power; RE, radiation efficiency; OE, overall efficiency; and D , directivity.



(a)



(b)

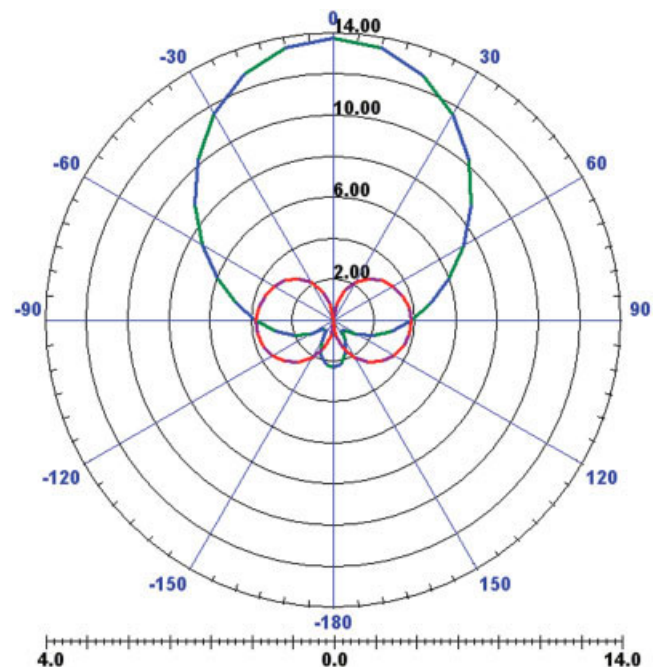
Figure 2 (a) Fabricated 2D EZ antenna, Design 2, mounted on a copper ground plane, and (b) corresponding HFSS predicted and measured S_{11} values. [Color figure can be viewed in the online issue, which is available at www.interscience.wiley.com]

We are currently investigating whether or not the structures that were designed to produce the capacitance in the current 2D and 3D designs can be replaced with lumped element capacitors to improve their overall efficiencies. A 2D planar antenna based on a lumped capacitor was considered using two L-shape “arms” being connected to the finite PEC ground plane and separated by a distance determined by the physical length of the lumped element capacitor. The width, length, and height of the L-shaped “arm” and the rectangular semiloop antenna were found to be (10, 35.75, 36.8 mm) and (10.4, 32, 6 mm) at 450 MHz, respectively. We used the MuRata high-Q MLCC, GJM1555C1H1R5JB01D, lumped element capacitor with a 1.5 pF capacitance for the designs and the experiments. Measured reflection coefficients showed a very good agreement with the simulated data and a detailed summary of these results will be reported elsewhere.

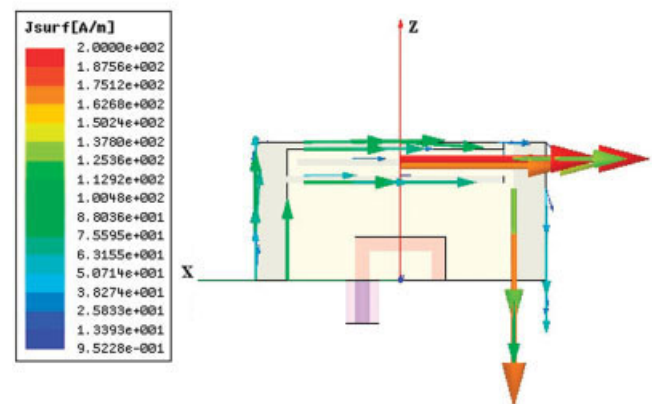
3. CONCLUSIONS

This research work reduces the earlier proposed three-dimensional EZ antenna system to a two-dimensional planar antenna design using a planar interdigitated CLL element. A 2D EZ

antenna is shown to be an attractive design because of its electrically-small size, yet easy-to-build and high overall efficiency characteristics. Because it is a highly resonant structure, the overall efficiency of the 2D antenna system depends on the choice of its overall electrical size. The versions of the EZ antenna system, whose sizes were near the electrically-small limit, were shown to be the most efficient. The conductor losses of the highly electrically-small versions were shown to dominate their overall efficiency. Far-field radiation and efficiency measurements of the 2D EZ antenna are currently in progress. In addition, a 2D EZ antenna design using a high-Q lumped element capacitor replacing the interdigitated capacitor fingers has been modeled, fabricated, and tested. This lumped element version has proven to be a competitive alternative to the model presented here and will be reported elsewhere.



(a)



(b)

Figure 3 (a) HFSS predicted far-field E- and H-field patterns, and (b) the surface current vectors on the interdigitated CLL element, obtained for Design 3 at the resonant frequency: 430.42 MHz. [Color figure can be viewed in the online issue, which is available at www.interscience.wiley.com]

ACKNOWLEDGMENT

This work was supported in part by DARPA contract number HR0011-05-C-0068.

REFERENCES

1. N. Engheta and R.W. Ziolkowski, A positive future for double negative metamaterials, *IEEE Microwave Theory Tech* 53 (2005), 1535–1556.
2. R.W. Ziolkowski and A. Erentok, Metamaterial-based efficient electrically small antennas, *IEEE Trans Antennas Propag* 54 (2006), 2113–2130.
3. A. Erentok and R.W. Ziolkowski, A hybrid optimization method to analyze metamaterial-based electrically small antennas, *IEEE Trans Antennas Propag*, in press.
4. A. Erentok and R.W. Ziolkowski, An efficient metamaterial-inspired electrically-small antenna, submitted to *Microwave Opt Technol Lett*.

© 2007 Wiley Periodicals, Inc.

MULTIFREQUENCY CHARACTERISTICS OF SINC SHAPED MICROSTRIP PATCH ANTENNA

Nisha Gupta, Mrinal Mishra, Suneel Chandra Kotha, and Yalamanchili Kiran

Department of Electronics and Communication Engineering, Birla Institute of Technology, Mesra, Ranchi 835 215 India

Received 28 November 2006

ABSTRACT: Characteristics of a single-layer, multi-frequency microstrip patch antenna, which uses a Sinc shaped microstrip patch configuration, are studied. This antenna is capable of providing good impedance matching at all frequencies without tuning the feed position and other design parameters. A parametric study is conducted using commercial software IE3D, based on method of moments (MoM) algorithm. The effects of various antenna parameters on resonant frequencies of the antenna are analyzed and discussed. Similar radiation patterns are obtained at three resonant frequencies. A prototype with dimensions based on the simulations is built and tested. A comparison between the measured and simulated results shows good agreement. © 2007 Wiley Periodicals, Inc. *Microwave Opt Technol Lett* 49: 1673–1675, 2007; Published online in Wiley InterScience (www.interscience.wiley.com). DOI 10.1002/mop.22541

Key words: microstrip antennas; multifrequency antennas; sinc shaped antennas

1. INTRODUCTION

Modern communication systems, such as, global positioning system, satellite digital audio radio service, wireless local area networks, and wireless personal area networks usually require antennas with compactness and low cost. They often require multiband operation and the requirement is obvious when the same antenna is required to support multiple applications. In addition, the multitude of different standards in cell phones and other personal mobile devices also require multi-band antennas. Therefore, the use of the same antenna for a number of different purposes, preferably in different frequencies is highly desirable.

Microstrip patch antennas [1] are very popular in wireless communication system applications. They offer an attractive way to integrate the RF front end of the system with its antenna and achieve a low profile, low weight, easy to fabricate, and low cost solution.

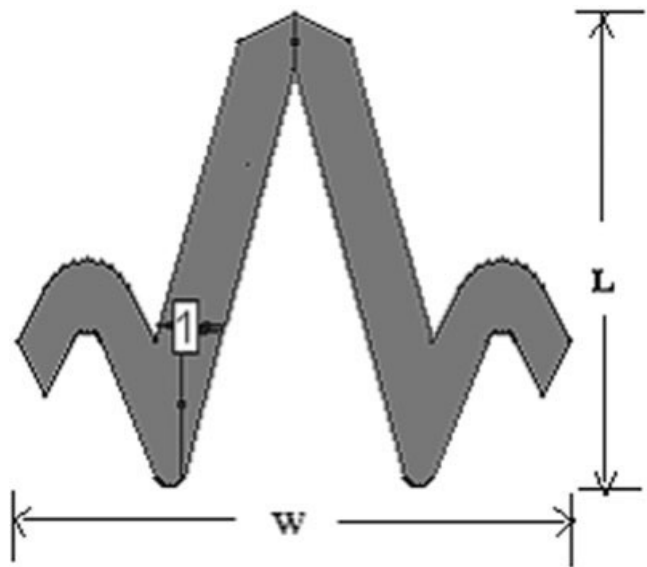


Figure 1 Sinc shaped microstrip patch antenna with feed position at 1

The Sinc shaped microstrip patch antenna proposed in this article operates at three different frequencies. It is fabricated on cheap dielectric material and offers a compact design suitable for integrating in mobile devices.

Ideally a multifrequency antenna should exhibit similar performances at all operating frequencies in terms of impedance and radiation pattern. There are quite a few techniques available currently to achieve multifrequency operation with microstrip antennas. The simplest way to operate a simple rectangular patch at dual bands is to use the first resonance of the two orthogonal dimensions of the rectangular patch, which are the TM₁₀₀ and TM₀₁₀ modes [2]. In this case, the frequency ratio is approximately equal to the ratio between the two orthogonal sides of the patch. Besides, multiple radiation elements [3] are also used for operation at multiple bands. Stacked arrangement of parasitic elements [4], coplanar arrangement of parasitic elements also exhibit multifrequency behavior. Another popular approach is the introduction of reactive loading to a single patch such as adoption of C-type, E-type, and H-type patches [5–7] and mounting of slots [8]. The solution to the need of multifrequency behavior can also be fulfilled by applying fractal concepts on microstrip antenna design-

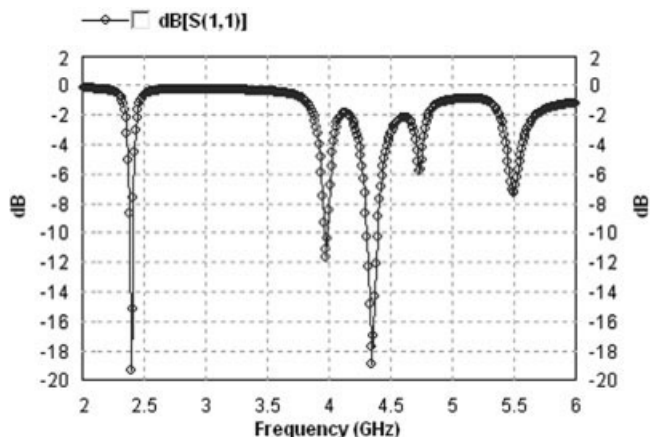


Figure 2 Simulated return loss characteristics showing multifrequency operation